6–35

Tanaka, Y., et al., 1995, Nature, 375, 659

Wilms, J., Reynolds, C. S., Begelman, M. C., Reeves, J., Molendi, S., Staubert, R., & Kendziorra, E., 2001, MNRAS, 328, L27

Ionization Equilibrium and Line Diagnostics

Introduction

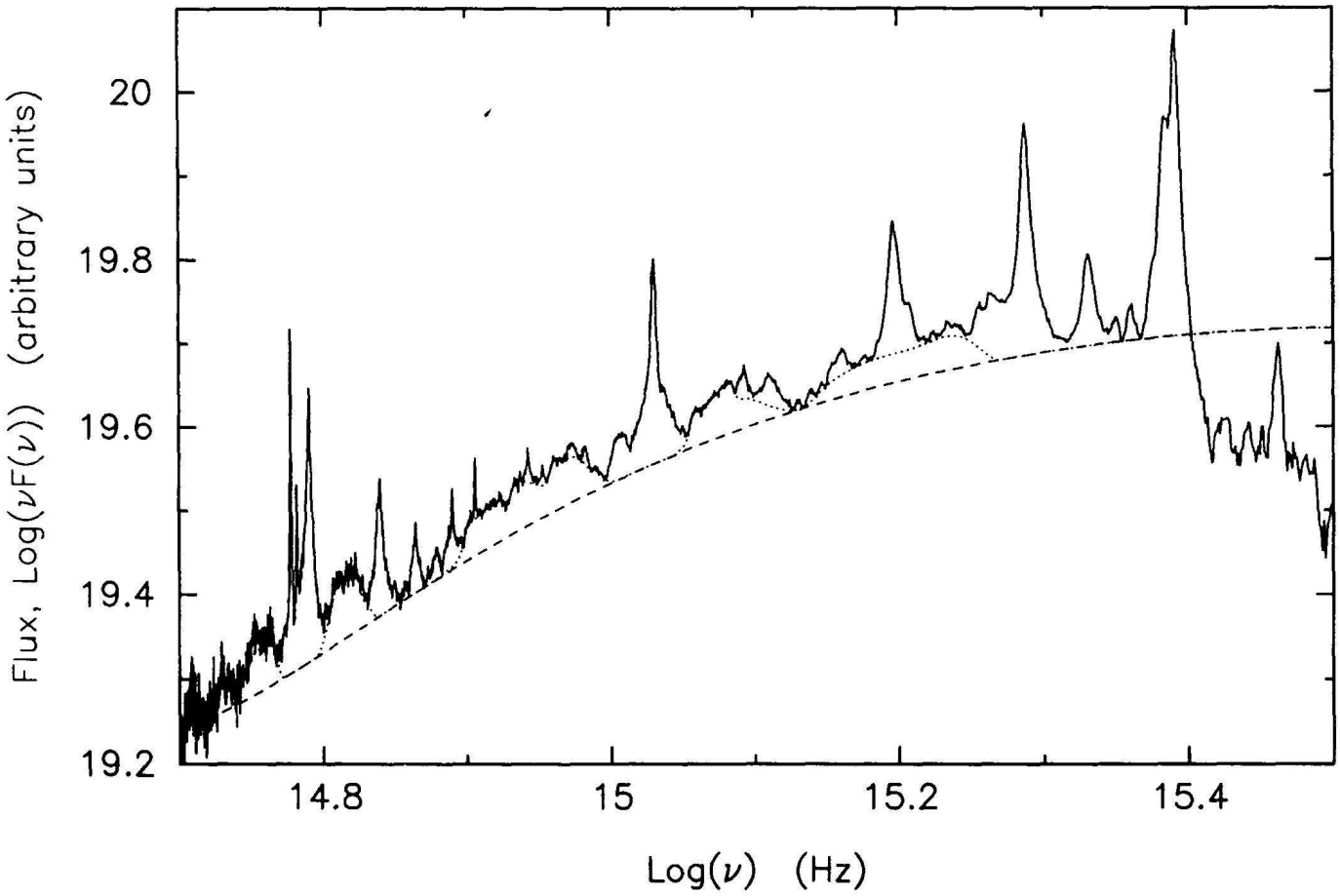

(average quasar spectrum Francis et al., 1991, Fig. 6)

Reminder: The average optical spectrum of AGN is dominated by broad and narrow lines.

Ionization Equilibrium, I

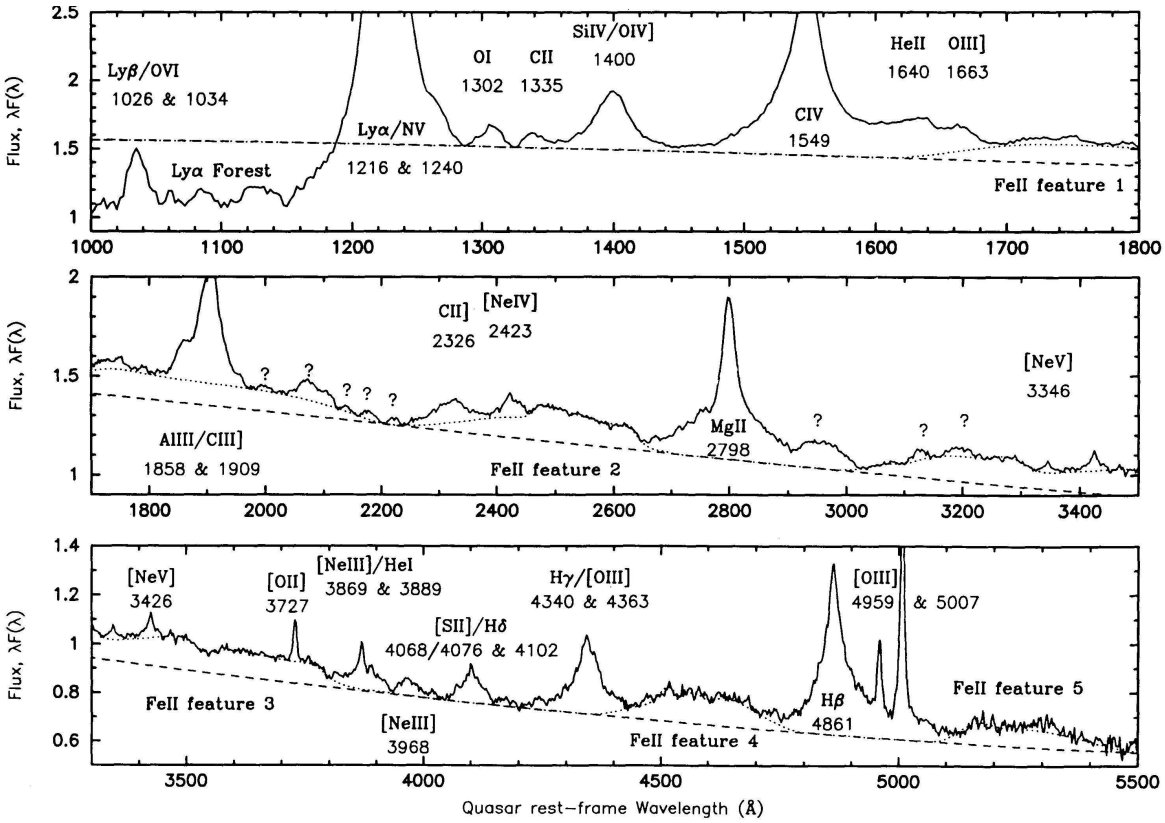

(average quasar spectrum
Francis et al., 1991, Fig. 7)

Typical spectra of AGN (and planetary nebulae) are dominated by Hydrogen lines, plus emission from O III at 5007 Å ("nebulium").

Physics: gas is in photoionization equilibrium with radiation of the vicinity of the central black hole.

TABLE 1

LINE STRENGTHS

Identification	Restframe Wavelength (Å)	Start[a] (Å)	End[a] (Å)	Relative Flux[b]	Standard Deviation	Equivalent Width (Å)	Note
Lyβ + O VI	1026 & 1034	1018	1054	9.3	...	5.3	
Lyα + N V	1216 & 1240	1186	1286	100	88	52	
O I	1302	1288	1325	3.5	...	1.9	
C II	1335	1325	1354	2.5	...	1.3	
Si IV + O IV]	1400	1353	1454	19	5	10	
C IV	1549	1452	1602	63	41	37	
He II + O III]	1640 & 1663	1602	1700	18	21	12	(1)
Al III + C III]	1858 & 1909	1828	1976	29	25	22	
2000 feature	...	1985	2018	0.49	...	0.42	
2080 feature	...	2035	2125	4.1	...	3.7	(2)
2140 feature	...	2125	2158	0.34	...	0.32	(3)
2175 feature	...	2158	2204	0.76	...	0.78	(4)
2200 dip?	...	...	...	...	...		(5)
2225 feature	...	2206	2238	0.47	...	0.51	
C II]	2326	2242	2388	6.0	...	6.4	
[Ne IV]	2423	2386	2464	2.2	...	2.39	(6)
Mg II	2798	2650	2916	34	20	50	(7)
2970 feature	...	2908	3026	6.3	...	10	(8)
3130 feature	...	3100	3156	0.73	...	1.3	
3200 feature	...	3156	3236	0.95	...	1.7	(9)
[Ne V]	3346	3324	3372	0.52	...	1.0	
[Ne V]	3426	3392	3452	1.0	...	2.1	
[O II]	3727	3712	3742	0.78	1.5	1.9	
[Ne III] + He I	3869 & 3889	3804	3934	3.6	...	9.8	(10)
[Ne III]	3968	3934	4012	1.3	...	3.9	
[S II] + Hδ	4068/4076 & 4102	4044	4148	2.8	...	8.9	
Hγ + [O III]	4340 & 4363	4276	4405	13	3.3	9.8	
Hβ	4861	4704	5112	22	4.1	58	
[O III]	4959	4942	4976	0.93	1.5	3.8	
[O III]	5007	4986	5044	3.4	3.6	15	
Fe II COMPONENTS:-							
1	...	1610	2210	46	18		
2	...	2210	2730	26	69		
3	...	2960	4040	39	23		(11)
4	...	4340	4830	11	8		
5	...	5050	5520	6.8	...		

[a] Wavelength limits between which the line flux was integrated.

[b] Percent of combined flux of Lyα + N v.

NOTES.—(1) Separation from C IV arbitrary; (2) Possible contribution from Fe II; (3) Possible contribution from N II λ2140; (4) Possible contribution from He II λ2186, but note that He II λ4686 is not seen; (5) Silicate dust absorption feature or gap in the Fe II emission?; (6) Flux and equivalent width calculated after a 20% correction for second-order Lyα contamination; (7) Blended with Fe II emission; (8) Possible contribution from Fe II; (9) Possible contribution from He II λ3203, but note absence of He II λ4686; (10) Continuum fitting particularly uncertain due to Balmer emission; (11) This component includes the Balmer continuum.

Strength of emission lines characterized by their equivalent width, defined by

$$\mathrm{EW} = \int_0^\infty \frac{f_{\mathrm{obs}}(\lambda) - f_{\mathrm{cont}}(\lambda)}{f_{\mathrm{cont}}(\lambda)}\, d\lambda \qquad (7.1)$$

units of EW: Å.

Similar definitions also also exist for E- or ν-space!

Rate Equations, I

Ionization structure of gas in AGN determined from the rate equations:

Atoms can be ionized and can recombine

$\Longrightarrow$ number density of ions can change with time.

Define

$n_Z(z)$: number density of species Z in ionization stage z (units: cm^{-3}).
$\lambda(z, z+1)$: transition rate from stage z to $z+1$ (units: s^{-1}).

then

$$\frac{\mathrm{d}n_Z(z)}{\mathrm{d}t} = n_Z(z-1)\lambda(z-1,z) - n_Z(z)(\lambda(z,z+1)+\lambda(z,z-1)) + n_Z(z+1)\lambda(z+1,z) \quad (7.2)$$

In equilibrium: $\mathrm{d}n_Z/\mathrm{d}t = 0$ and thus

$$\frac{n_Z(z+1)}{n_Z(z)} = \frac{\lambda(z,z+1)}{\lambda(z+1,z)} \quad (7.3)$$

In Eq. (7.2) only adjacent ionization stages are connected, calculation gets (much) more complicated if also z, $z+2$, etc. are connected.

Rate Equations, II

The rate equations are determined from all physical processes with result in ionization or recombination.

- Most important processes for ionization:
  - Photoionization
  - Collisional Ionization
- Most important processes for recombination:
  - Radiative Recombination
  - Dielectronic Recombination

We will now look at the physics of these processes in greater detail.

Photoionization, I

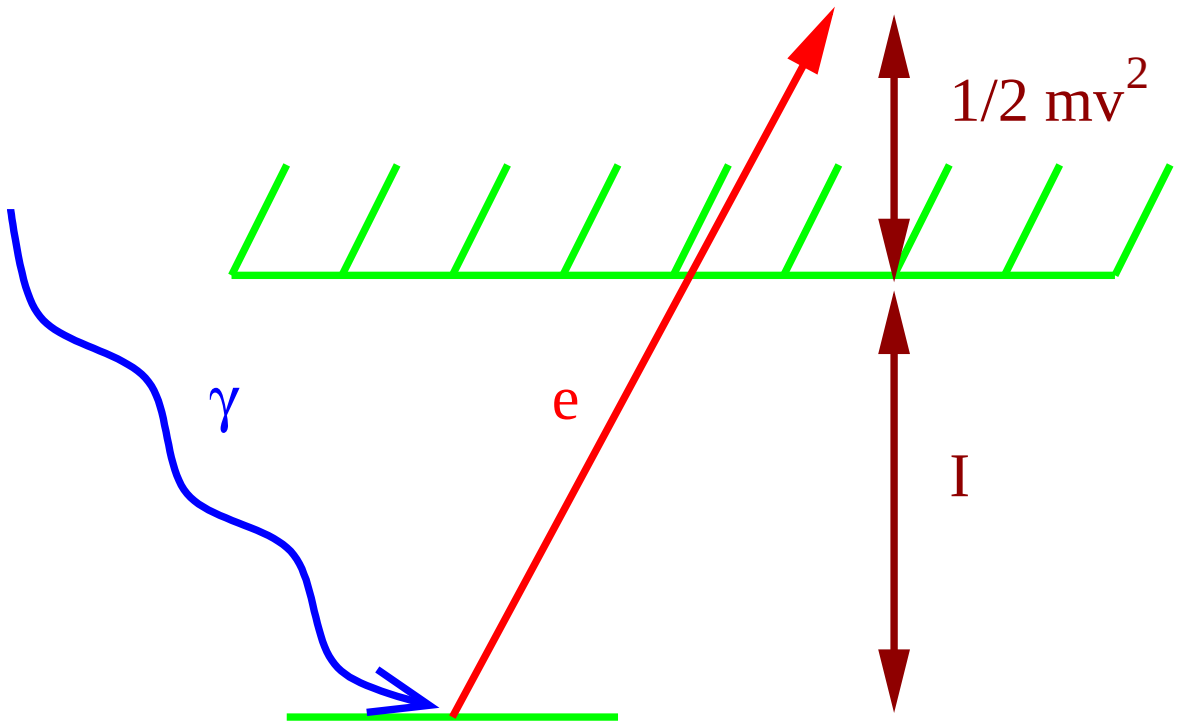

Photoionization: Ionization of an ion by a photon.

Reaction equation:

$$(Z, z) + \gamma \longrightarrow (Z, z+1) + \mathrm{e}^-$$

Photon needs energy $h\nu >$ ionization energy $I =: h\nu_{\mathrm{thresh}}$, remaining energy, $h\nu - I$, goes into kinetic energy of electron and is thermalized

Photoionization rate:

$$\gamma_\gamma(z, z+1) = \Gamma_{Z,z} = \int_{\nu_{\mathrm{thresh}}}^{\infty} \frac{F_\nu}{h\nu} \sigma_{\mathrm{bf}}(\nu) \mathrm{d}\nu \tag{7.4}$$

where σ_{bf}: photoionization cross-section ("bf": bound-free).

Photoionization, II

$\sigma_{\rm bf}$ is determined by quantum mechanics.

For Hydrogen, for absorption from the nth level (Menzel & Pekeris, 1935):

$$\sigma_{\rm bf} = \left(\frac{64\pi^4 m_{\rm e} e^{10}}{3\sqrt{3}ch^6}\right) \frac{1}{n^5\nu^3} g_{\rm bf}(n,\nu) \propto \frac{1}{\nu^3} \tag{7.5}$$

where the Gaunt-factor, $g_{\rm bf}$, is tabulated, e.g., by Karzas & Latter (1961) and is $\propto \nu^{-1/2}$ away from threshold.

For the ground state of hydrogen:

$$g_{{\rm bf};1,\nu} = 8\pi\sqrt{3}\frac{\nu_1}{\nu}\frac{e^{-4z\,\cot^{-1}z}}{1-e^{-2\pi z}} \tag{7.6}$$

where $z^2 = \nu_1/(\nu-\nu_1)$ and where $h\nu_1$ is the binding energy of Hydrogen.

Useful fitting formulae for all elements and ions with $Z \leq 30$ have been published by Verner & Yakovlev 1995 and Verner et al. 1996, detailed calculations have been performed by the opacity project (TOP, Seaton et al.).

Photoionization, III

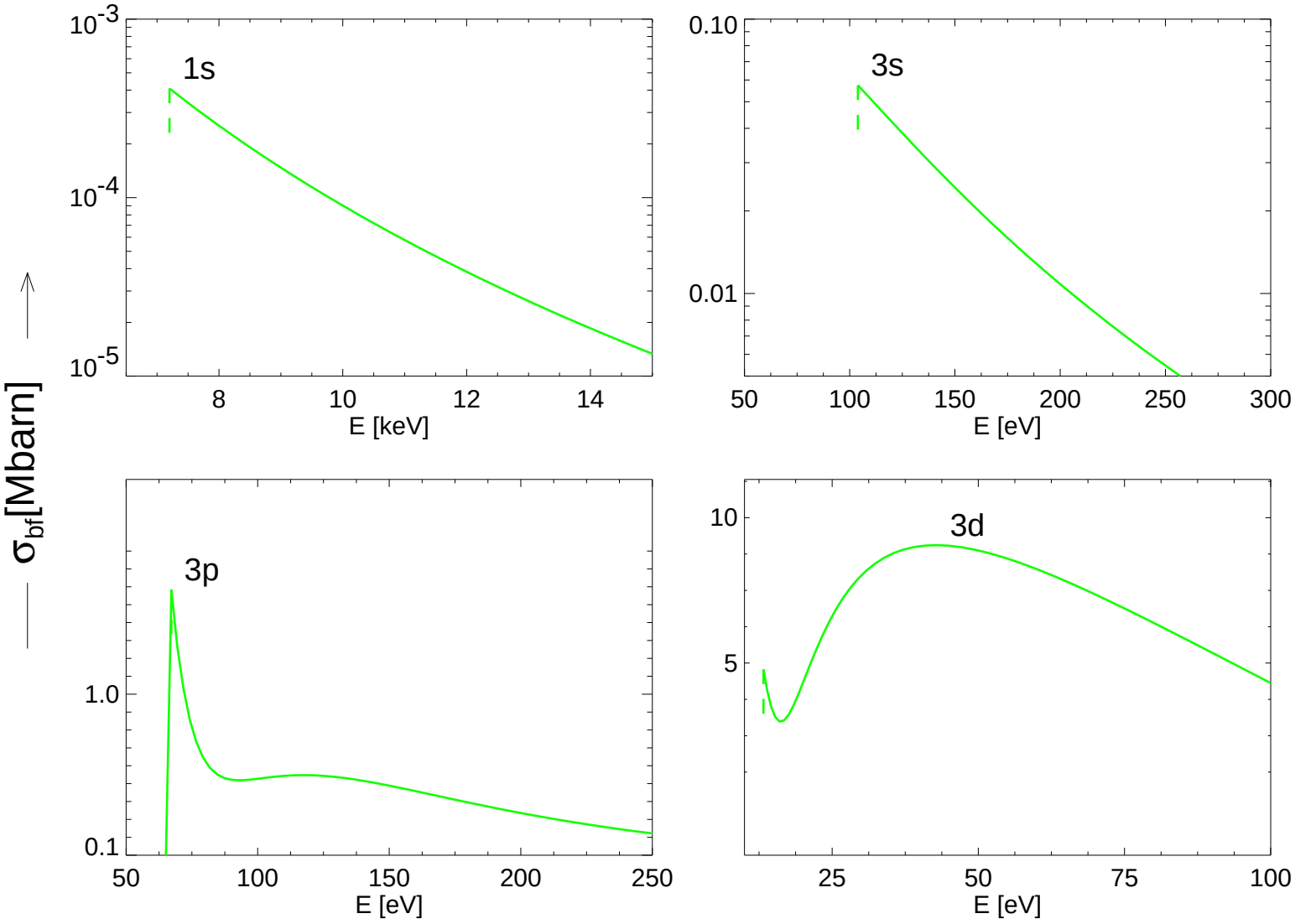

Photoionization cross sections for several subshells of Fe (cross sections from Verner et al., 1996).
1 barn = 10^{-24} cm^2.

Photoionization, IV

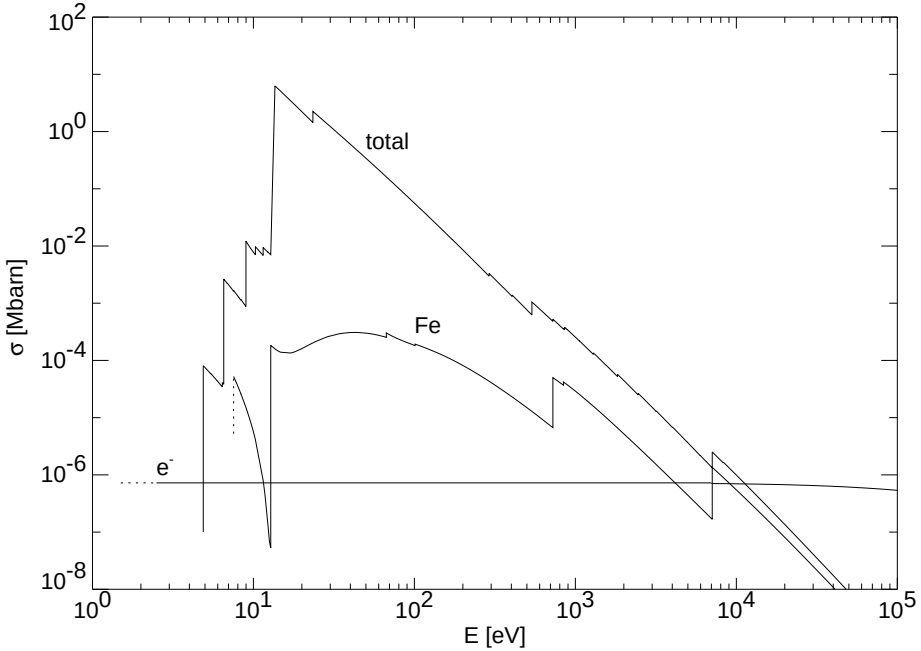

$\sigma_{\rm bf}$ per H-atom for material of solar composition from the optical to the X-ray regime.

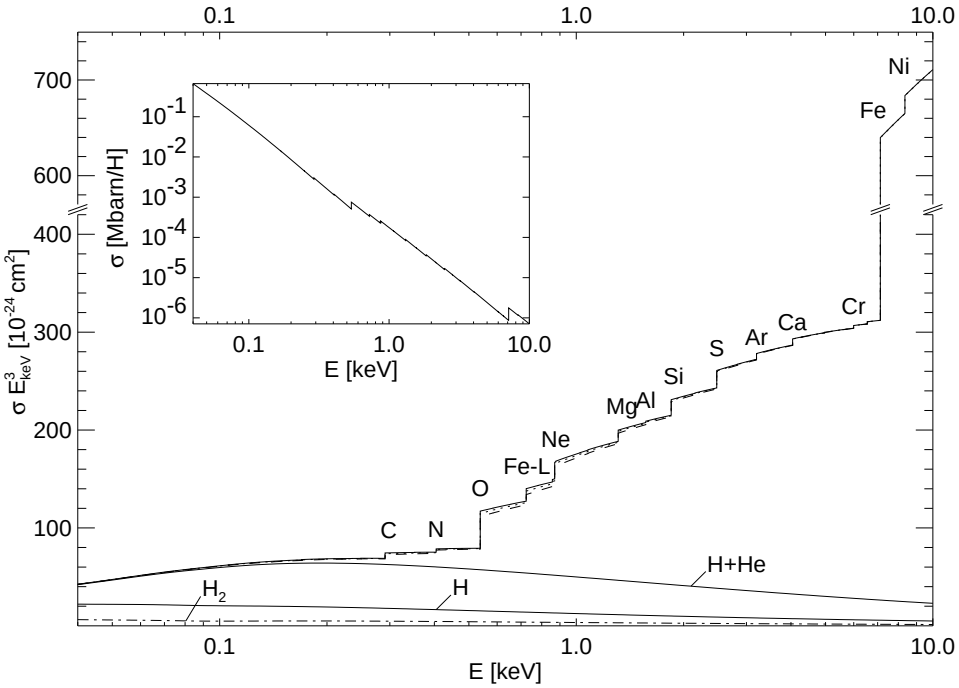

$\sigma_{\rm bf}E^3$ in the EUV and X-rays (dashed: influence of dust), Wilms, Allen & McCray (2000).

Note strong E^{-3} dependency above the absorption edges!

In the X-rays, most of the absorption is *not* from hydrogen, although absorbing columns are still given in terms of an equivalent hydrogen column, $N_{\rm H}$.

Photoionization, V

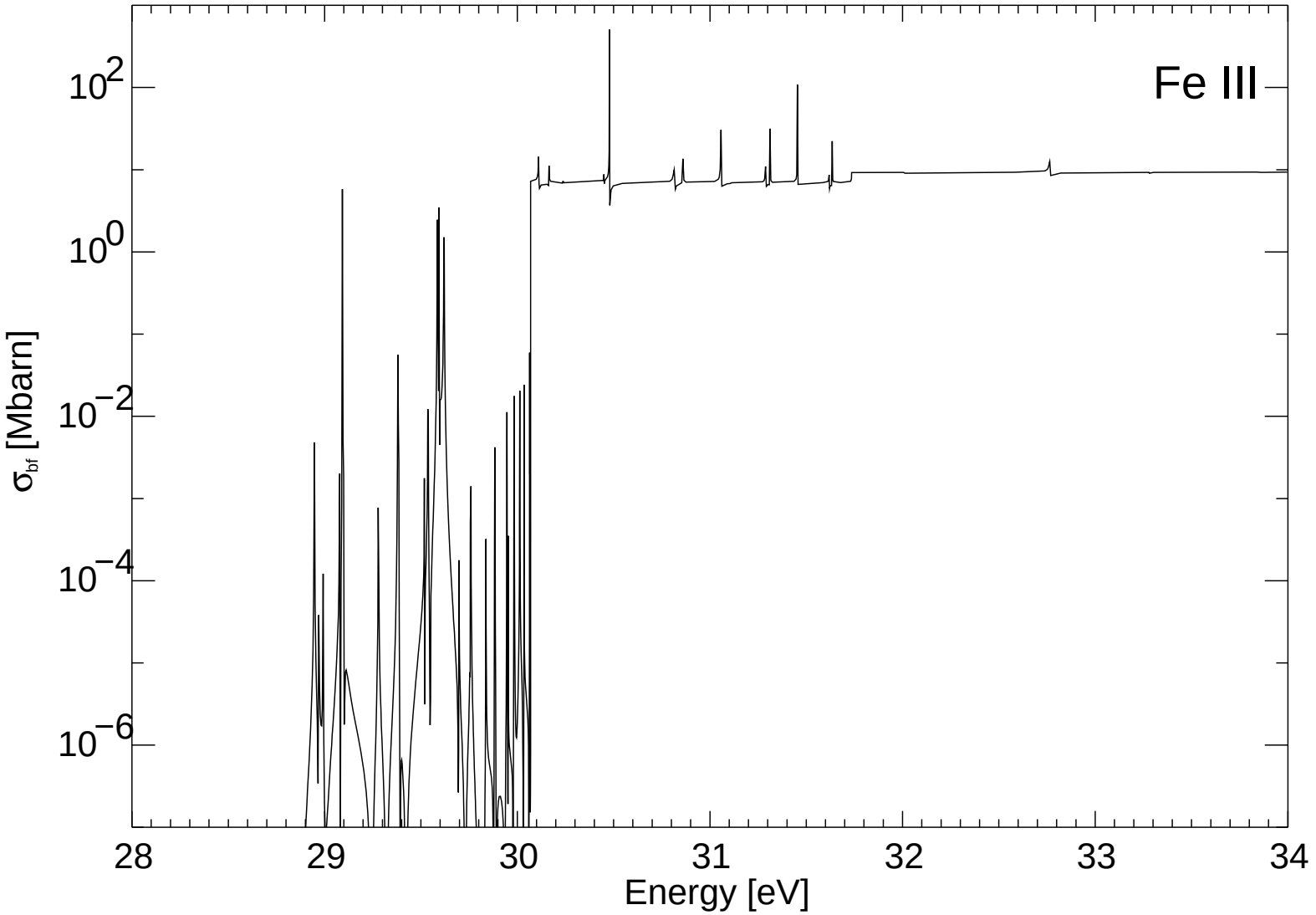

TOP cross-section for Fe III

Photoionization, VI

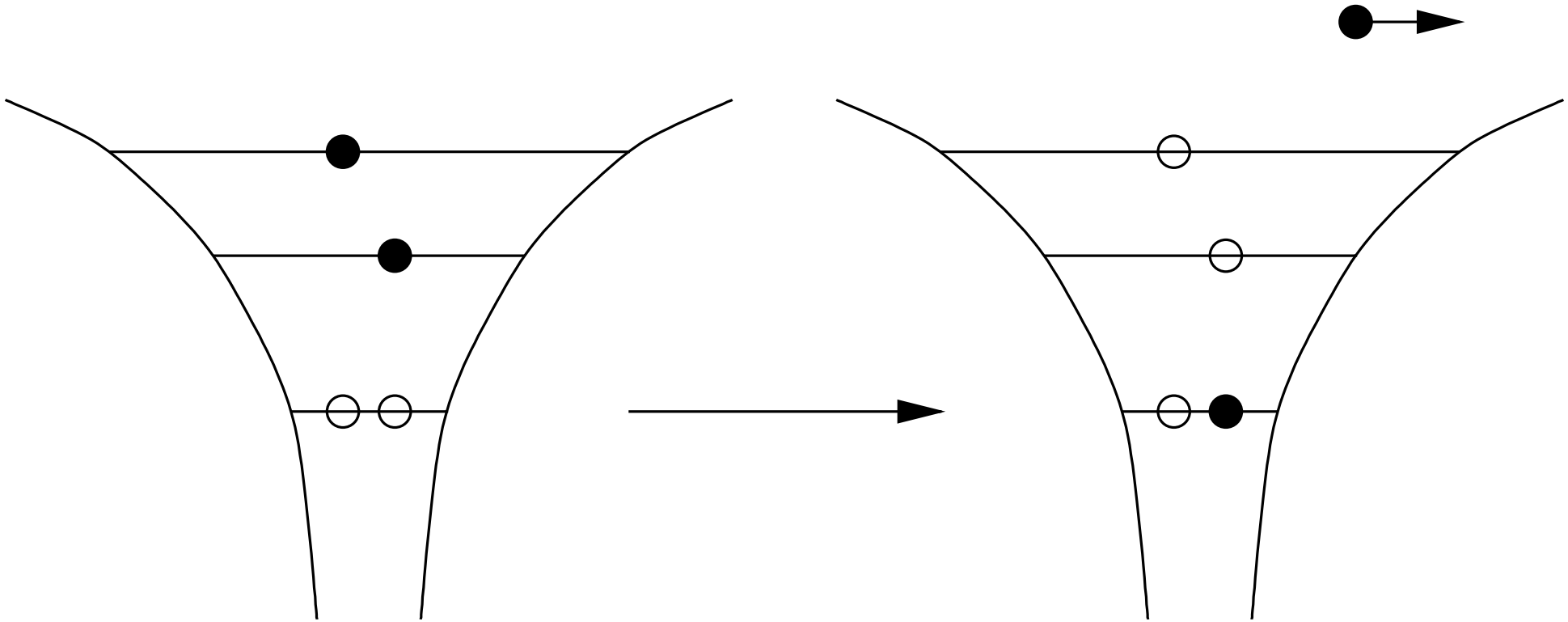

Resonance structure close to ionization threshold: σ_{bf} is influenced by autoionization resonances, where more than one electron is involved.

Collisional Ionization, I

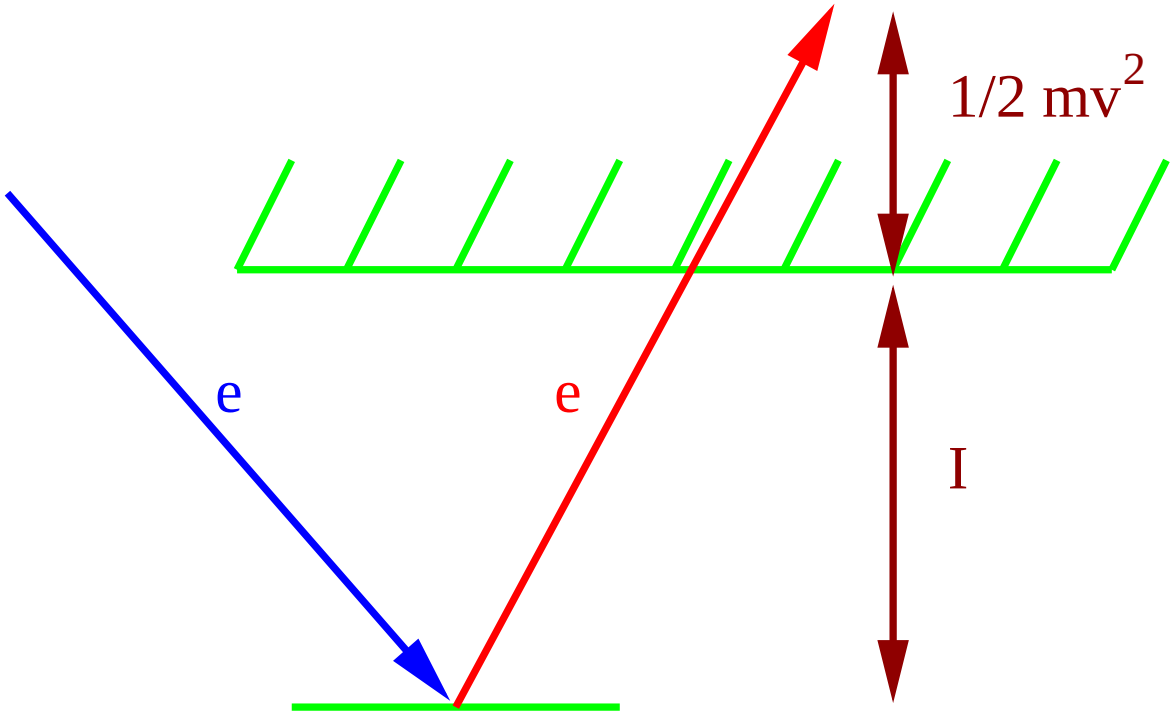

Collisional Ionization:
Ionization of an ion by a collision with an electron.

Reaction equation:

$$(Z,z)+\mathrm{e}^- \longrightarrow (Z,z+1)+\mathrm{e}^-+\mathrm{e}^-$$

Collisional Ionization rate depends on the electron velocity distribution:

$$\gamma_{\mathrm{coll.}}(z,z+1) = n_{\mathrm{e}} C_Z(z,T_{\mathrm{e}}) = n_{\mathrm{e}} \int_{v_{\mathrm{thresh}}}^{\infty} \sigma_i(v) v f(v) \mathrm{d}^3 v =: n_{\mathrm{e}} \langle v\sigma_i \rangle \qquad (7.7)$$

where σ_{i} is the collisional ionization cross-section, and C_Z is the collisional ionization rate coefficient (units cm^{3}s).

In AGN one typically assumes $f(v)$ to be a Maxwell distribution.

Collisional Ionization, II

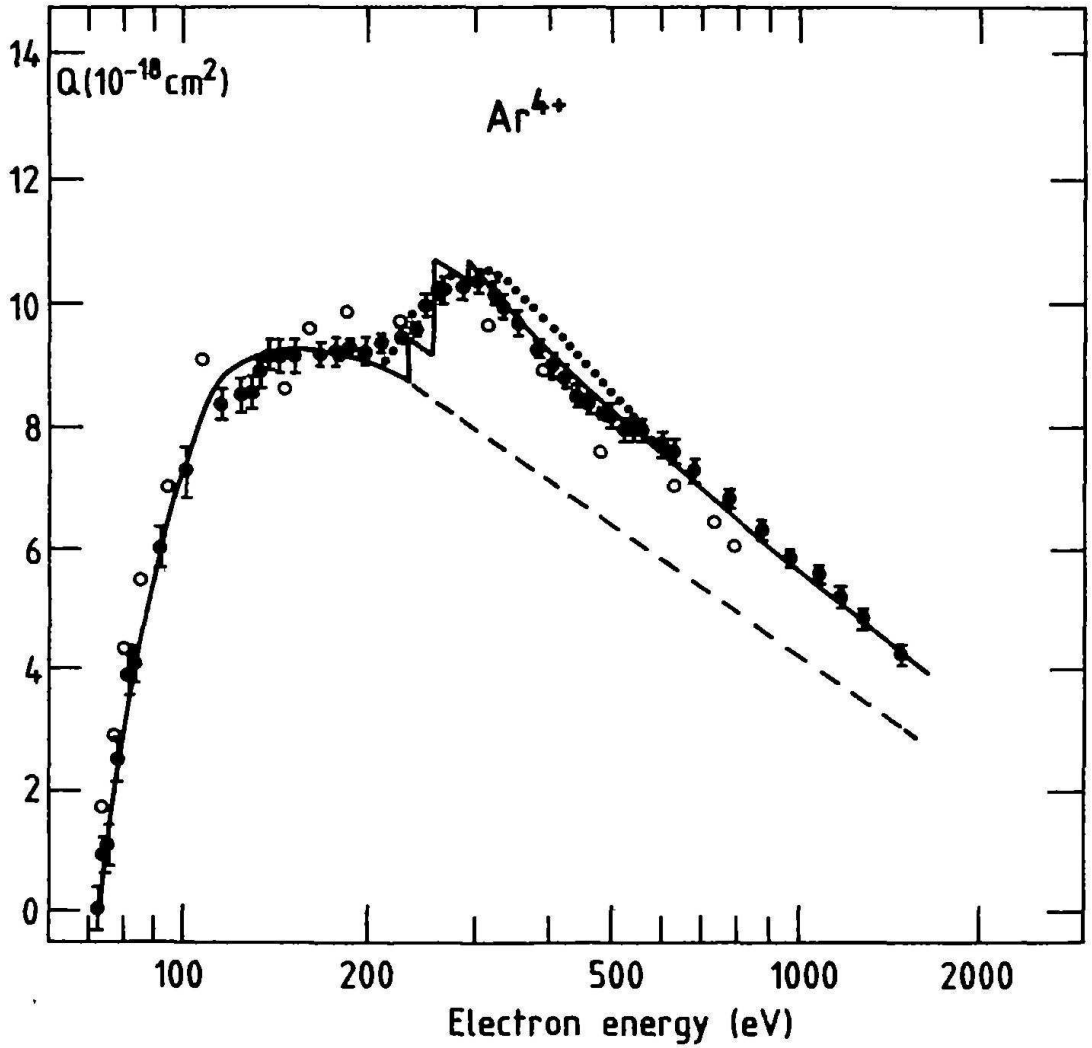

$\sigma_i(v)$ for Ar IV (Arnaud & Rothenflug, 1985, Fig. 8)

C_Z is normally presented in tabulated form, a typical fitting formula is:

$$C_Z(z,T) = A_z T^{1/2} \frac{\exp(-I/kT)}{1 + a_z(T/T_Z)} \tag{7.8}$$

where $T_Z = I/kT$.

See, e.g., Arnaud & Rothenflug (1985) or Shull & Van Steenburg (1982).

Radiative Recombination, I

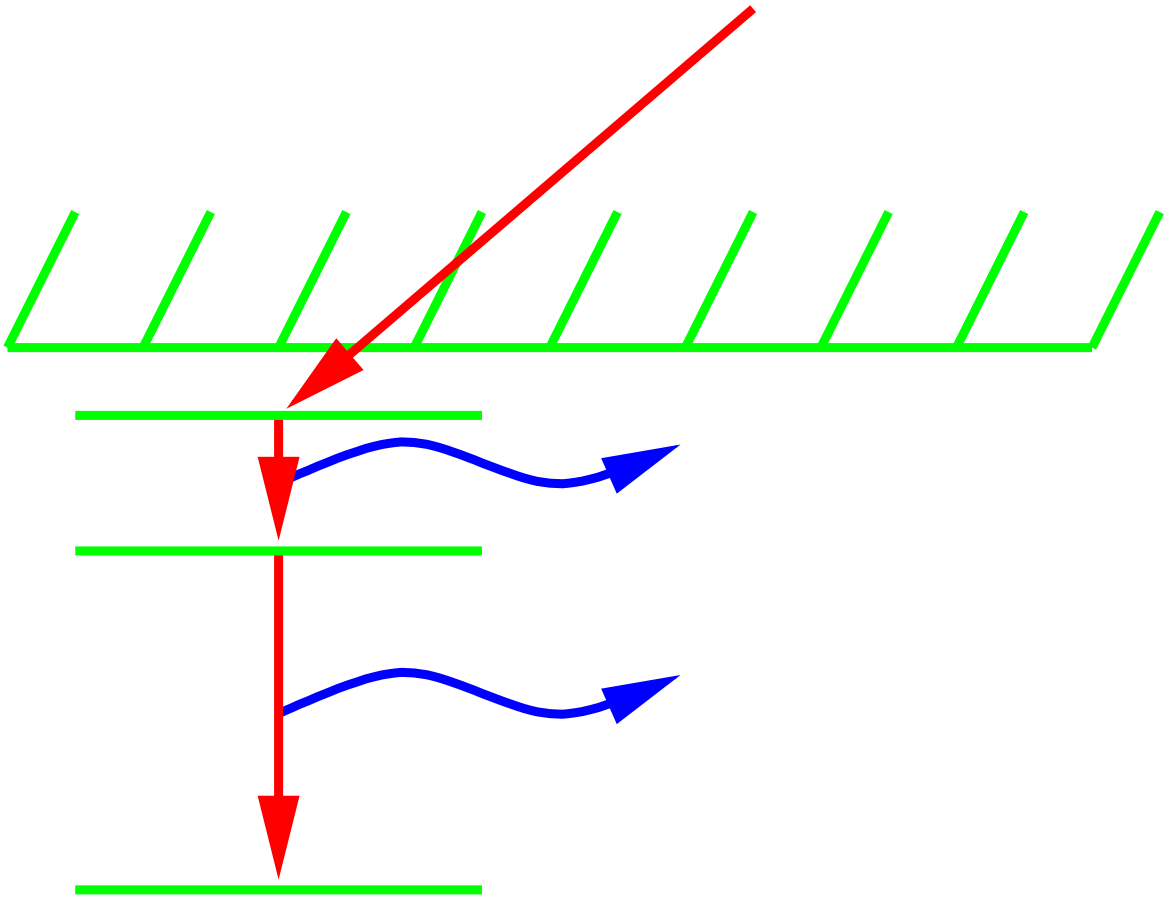

Radiative Recombination:
Capture of an electron into the excited state of an ion with subsequent radiative cascade to ground state.

Reaction equation:

$$(Z, z{+}1){+}\mathrm{e}^- \longrightarrow (Z, z){+}\gamma{+}\gamma{+}\ldots$$

Recombination rate:

$$\lambda_{\mathrm{fb}} =: n_{\mathrm{e}} \alpha_{Z,z}(T) = n_{\mathrm{e}} \int_0^\infty \sigma_{\mathrm{fb}}(v) v f(v) \mathrm{d}^3 v =: n_{\mathrm{e}} \left\langle \sigma_{\mathrm{fb}} v \right\rangle \qquad (7.9)$$

Radiative Recombination, II

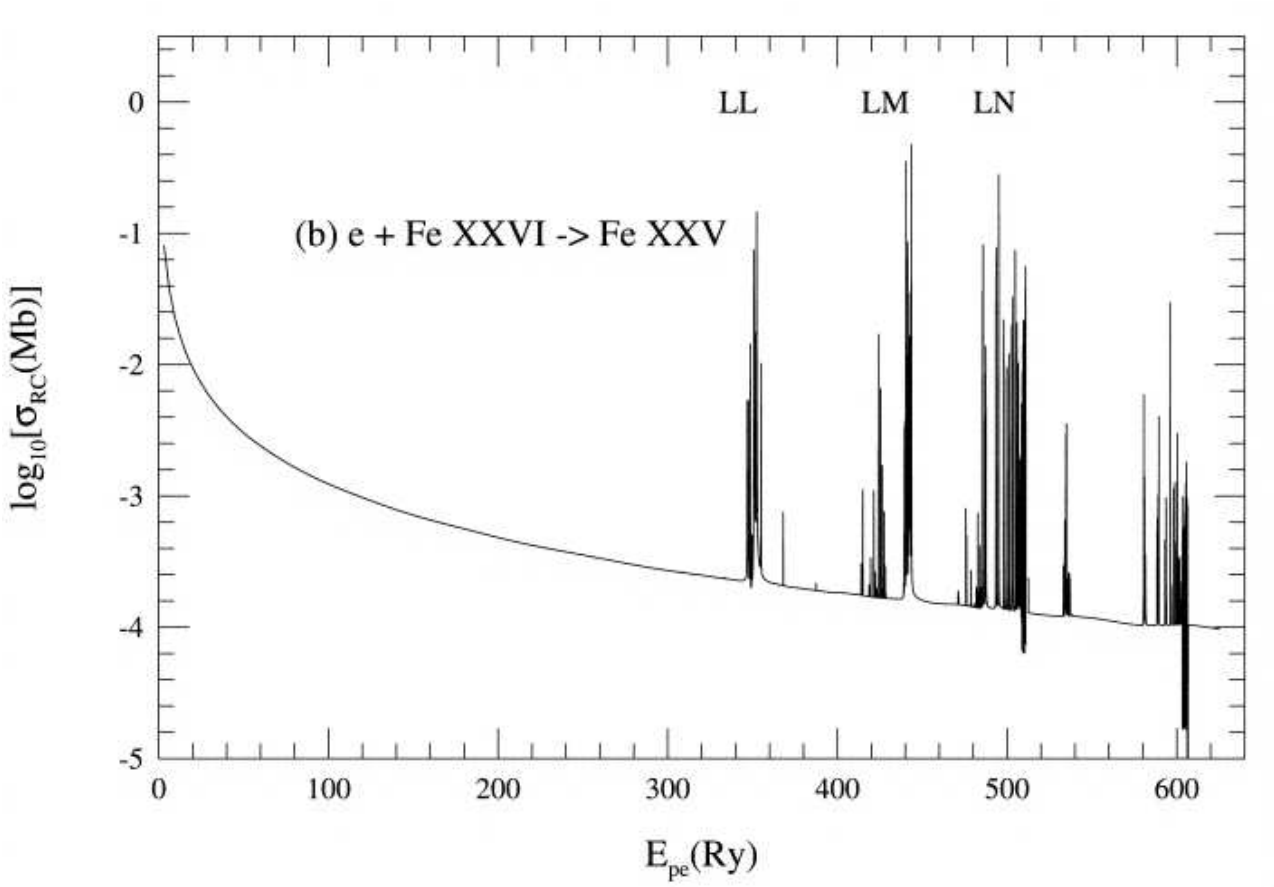

(Nahar, Pradhan & Zhang, 2001, Fig. 3)

The recombination cross-section, σ_{fb}, can be obtained from the photoabsorption cross-section, σ_{bf} using the Milne relation (see handout),

$$\sigma_{\mathrm{fb}}(v) = \frac{g_{z,n}}{g_{z+1,1}} \frac{h^2\nu^2}{m_{\mathrm{e}}^2 c^2 v^2} \sigma_{\mathrm{bf}}(\nu) \qquad (7.10)$$

The cross-section for recombination, σ_{fb}, can be easily derived using the principle of detailed balance. The derivation given here follows Osterbrock (1989).

The microphysical processes that are balanced are photoionization by photons in the energy range from $h\nu$ to $h(\nu + \mathrm{d}\nu)$ on the one hand, and (spontaneous or induced) recombinations from electrons in the velocity range from v to $v + \mathrm{d}v$ on the other hand. Thus, v and ν are related by

$$\frac{1}{2} m_{\mathrm{e}} v^2 + h\nu_{\mathrm{thresh}} = h\nu \tag{7.11}$$

$$m_{\mathrm{e}} v \mathrm{d}v = h \mathrm{d}\nu \tag{7.12}$$

In thermodynamical equilibrium, the rate of induced recombinations is $\exp(-h\nu/kT_{\mathrm{e}})$ times the rate of induced ionizations (this is the "detailed balance", such that

$$n_{\mathrm{e}} n_{Z,z+1} v \sigma_{\mathrm{fb}}(v) f(v)\, \mathrm{d}v = (1 - \exp(-h\nu/kT_{\mathrm{e}}))\, n_{Z,z} \frac{4\pi B_\nu(T_{\mathrm{e}})}{h\nu} \sigma_{\mathrm{bf}}(\nu) \mathrm{d}\nu \tag{7.13}$$

Because we are in thermodynamical equilibrium, the radiation fi eld is a Planckian, B_ν, and the electron distribution, $f(v)$, is given by the Maxwell-Boltzmann distribution,

$$f(v) = \frac{4}{\sqrt{\pi}} \left(\frac{m_{\mathrm{e}}}{2kT_{\mathrm{e}}} \right)^{3/2} v^2 e^{-m_{\mathrm{e}} v^2 / 2kT_{\mathrm{e}}} \tag{7.14}$$

As is shown in many introductory books to astrophysics, in thermodynamical equilibrium the ionization structure is given by the Saha equation,

$$\frac{n_{Z,z+1} n_{\mathrm{e}}}{n_{Z,z}} = \frac{2 g_{z+1}}{z_i} \left(\frac{2\pi m_{\mathrm{e}} kT_{\mathrm{e}}}{h^2} \right)^2 e^{-h\nu_{\mathrm{thresh}}/kT_{\mathrm{e}}} \tag{7.15}$$

where the g_i are the statistical weights of the two ionization stages.

Inserting everything gives the Milne relation

$$\sigma_{\mathrm{fb}}(v) = \frac{g_{z,n}}{g_{z+1,1}} \frac{h^2 \nu^2}{m_{\mathrm{e}}^2 c^2 v^2} \sigma_{\mathrm{bf}}(\nu) \tag{7.10}$$

for the recombination cross section σ_{fb} into the nth level of the ion (Z, z). Here, we've explicitly written down the statistical weight of this level as $g_{z,n}$ and assumed that the recombining ion, $(Z, z+1)$ is in its ground state ($n = 1$).

An alternative derivation using quantum mechanics uses symmetry arguments for the relevant matrix elements $\langle z|H|z+1\rangle$.

Dielectronic Recombination

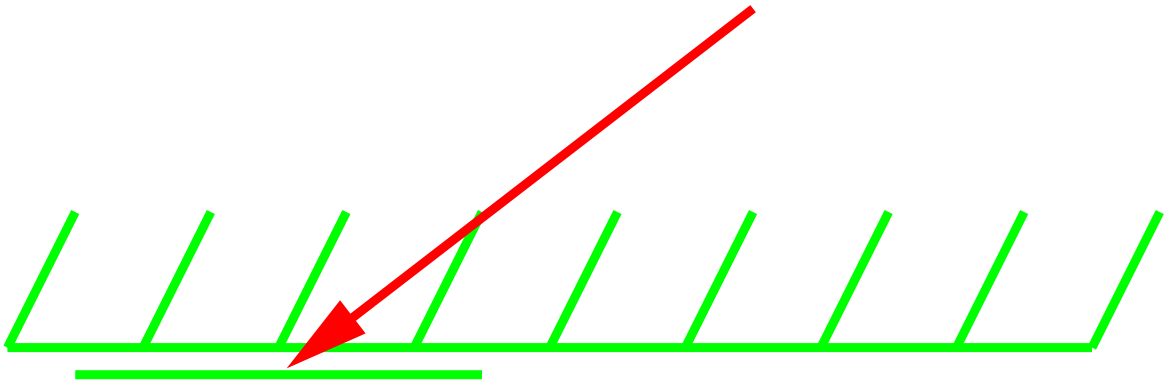

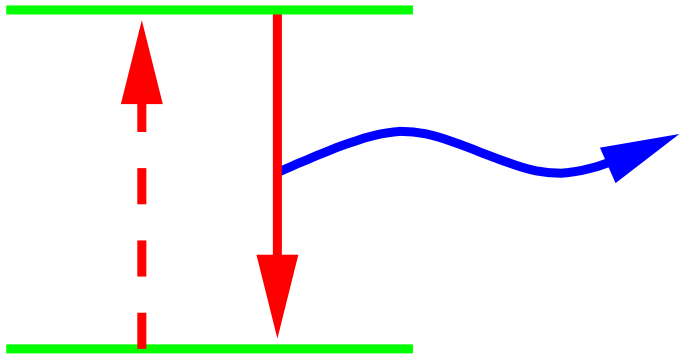

Dielectronic Recombination:
Capture of electron into excited Rydberg state, followed by radiative stabilization.

Reaction equation:

$$(Z, z+1) + \mathrm{e}^- \longrightarrow (Z, z+1)^* \longrightarrow (Z, z) + \gamma + \ldots$$

Since *two* electrons are excited $\Longrightarrow$ dielectronic recombination leads to emission of satellite lines, important, e.g., in solar corona and in photoionized gases around X-ray binaries, less so in AGN.

Photoionization

Assume: cloud irradiated by photons

Simplification: only source for ionization: photoionization

Equilibrium: number ionizations $=$ number of recombinations $\Longrightarrow$

$$\int_{\nu_{\text{ion}}}^{\infty} n(Z^z)\sigma_{\text{bf}}(\nu)\frac{F_\nu}{h\nu}\text{d}\nu = \alpha(T)n_{\text{e}}n(Z^{z+1}) \tag{7.16}$$

where

$\sigma_{\text{bf}}(\nu)$: photoionization cross section (cm^2; $\propto E^{-3}$)

$\alpha(T_{\text{e}})$: total recombination coeffi cent (cm^3 s^{-1})

n_i: particle density (cm^{-3})

F_ν: local photon flux (erg cm^{-2} s^{-1} keV^{-1})

where F_ν is related to the source luminosity via

$$F_\nu = \frac{L_\nu}{4\pi D^2} \tag{7.17}$$

Photoionization

Since $\sigma_{\rm bf}(\nu)$ is a strongly peaked function, we can write Eq. (7.16) as

$$n(Z^z)\sigma_{\rm bf}(\nu_{\rm ion})\frac{F_{\nu_{\rm ion}}}{h\nu_{\rm ion}} \sim \alpha(T) n_{\rm e} n(Z^{z+1}) \tag{7.18}$$

and therefore

$$\frac{n(Z^{z+1})}{n(Z^z)} \sim \frac{\sigma_{\rm bf}(\nu_{\rm ion})}{\alpha(T)} \frac{L}{4\pi D^2 n_{\rm e}} \frac{1}{h\nu_{\rm ion}} \tag{7.19}$$

i.e., ionization equilibrium mainly depends on

$$U = \frac{L/4\pi D^2 h\nu_{\rm ion}}{n_{\rm e}} \frac{1}{c} = \frac{\#\ \text{ionizing photons/cm}^3}{\#\ \text{electrons/cm}^3} \tag{7.20}$$

where U is called the ionization parameter

many other definitions available!

Example: For the BLR: $D \sim 10$ light days, $L/h\nu \sim 10^{51}$ photons, and $n = 10^{11}\,\text{cm}^{-3}$ gives $U \sim 0.1$.

Photoionization

In reality, as shown before many radiative processes need to be considered:

Ionization:

- Photoionization
- collisional Ionization
- Auger-Ionization

Recombination:

- radiative recombination
- dielectric recombination

Continuum Processes:

- Bremsstrahlung
- Compton-Scattering

Real life: Solution using advanced radiation codes such as Cloudy or XSTAR (it is *not* worthwhile to develop your own code. . .).

Photoionization

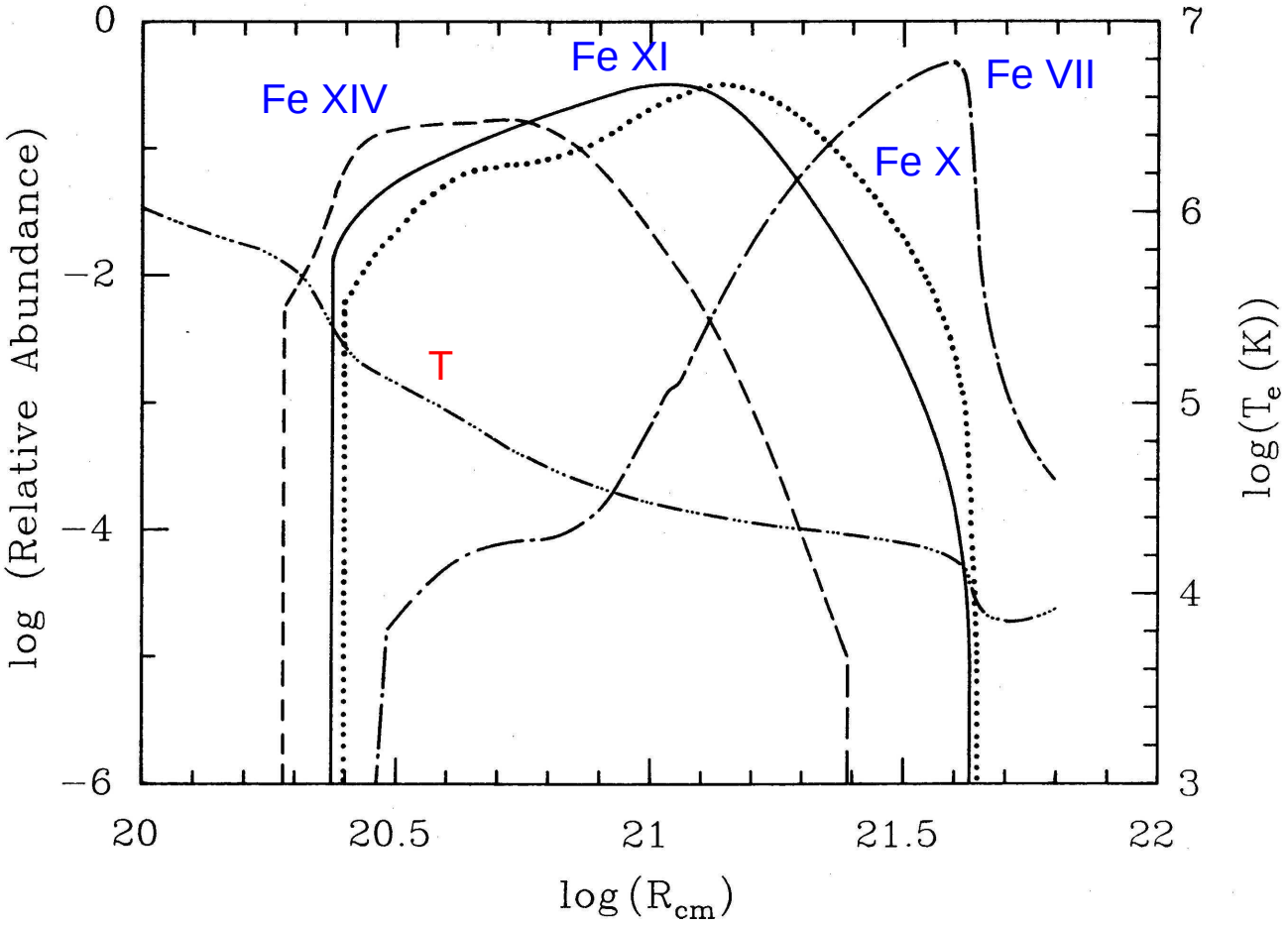

(Korista & Ferland, 1989, Fig. 5)

Fe ionization structure and temperature profile of a cloud with $n_{\mathrm{H}} = 1\,\mathrm{cm}^{-3}$ as a function of distance from a central source with a typical AGN continuum.

Photoionization

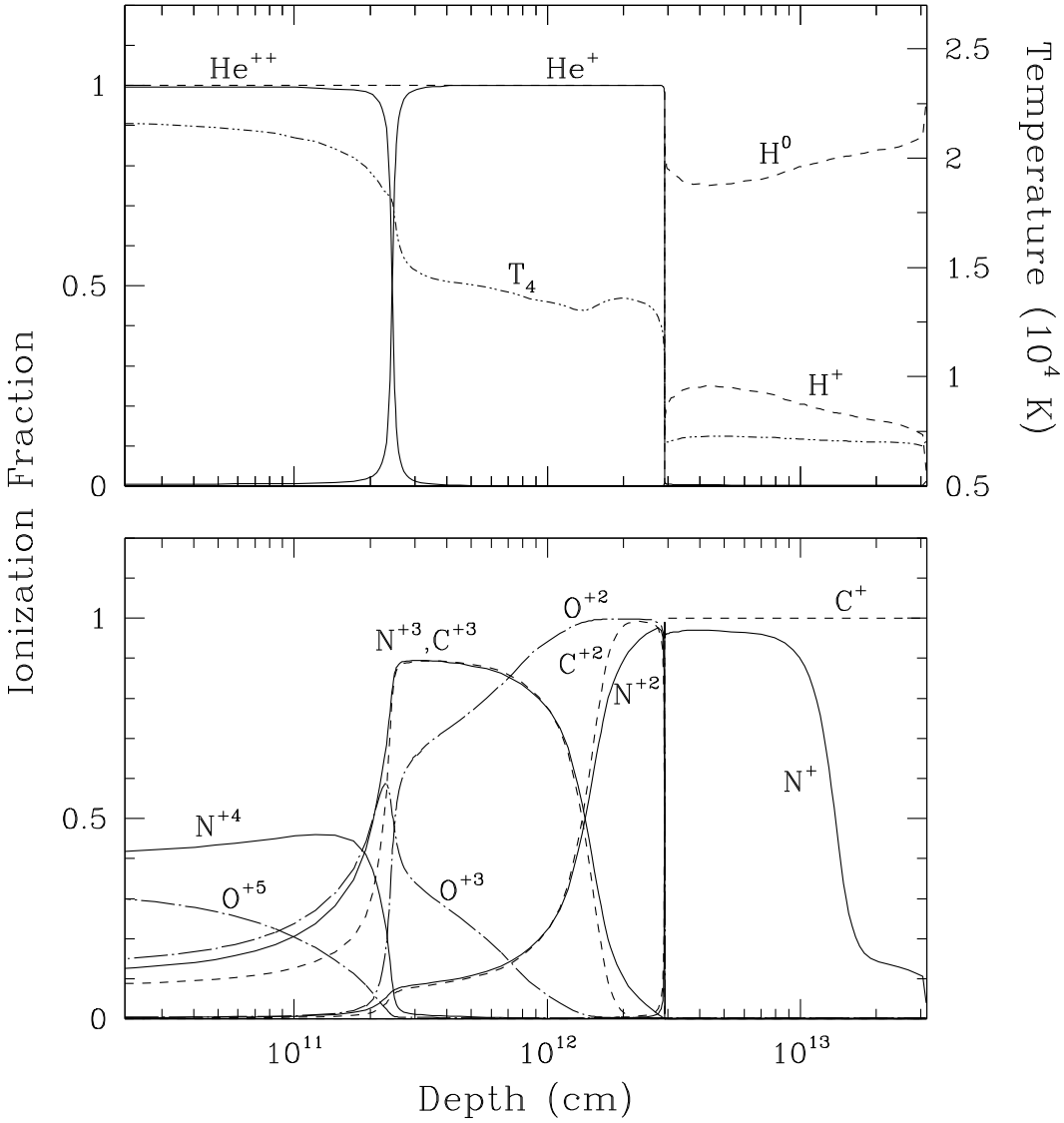

"Strömgren sphere" like structure of a cloud irradiated with a typical AGN spectrum (Mathews & Ferland, 1987) with $U = 0.1$, and $n_{\mathrm{H}} = 10^{10}\,\mathrm{cm}^{-3}$ (typical for BLR).
Distance is "into" cloud.

(Hamann et al., 2002, Fig. 1)

Photoionization

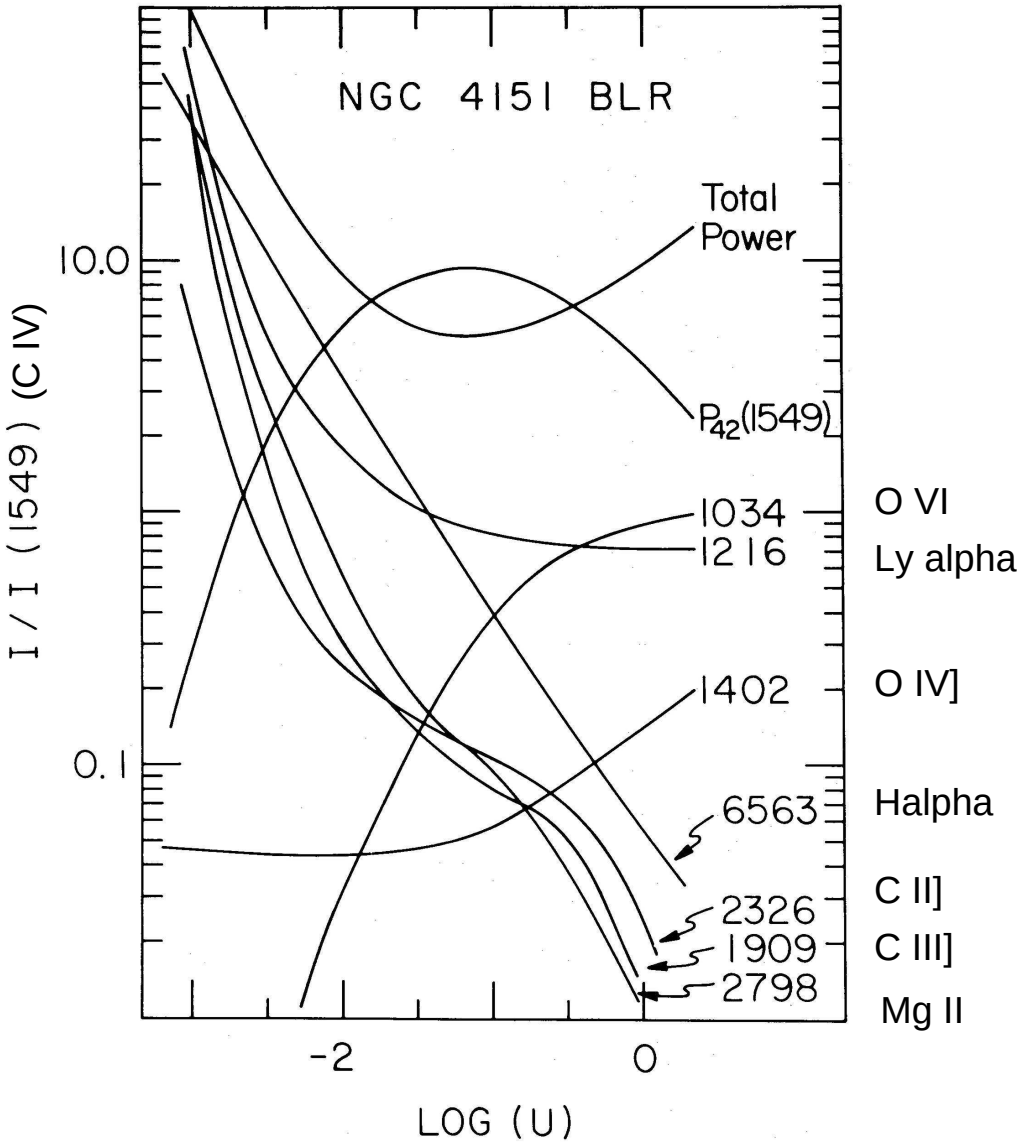

Line ratios of prominent lines with respect to C IV 1549Å as a function of the ionization parameter for parameters appropriate to the BLR in NGC 4151.

$P_{42}(1549)$: Total power emitted in C IV-line.

Note that C IV line carries $\sim$15% of the total flux! $\Longrightarrow$ can be used to estimate bolometric flux!

(Ferland & Mushotzky, 1982, Fig. 5)

Photoionization

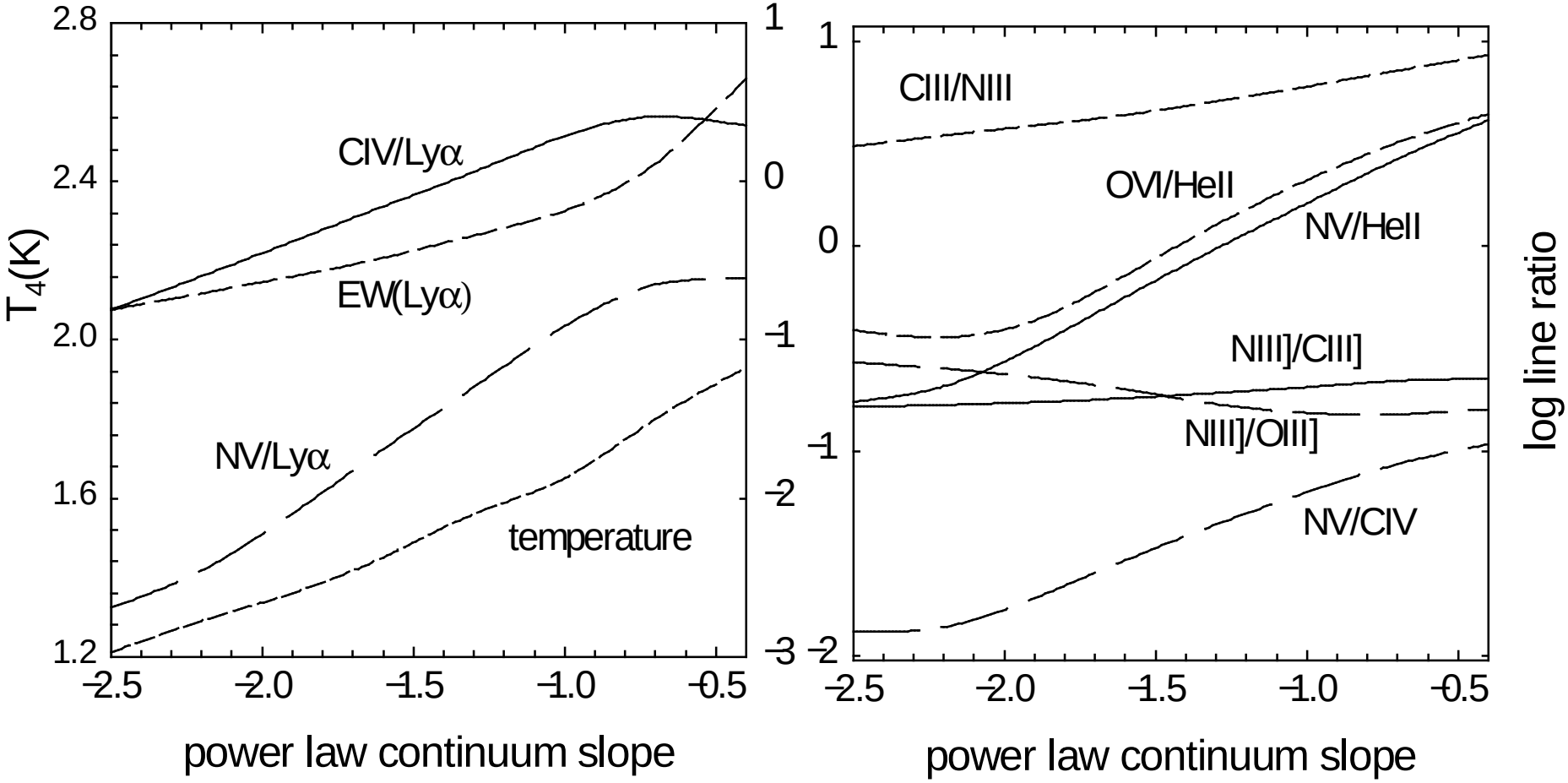

(Hamann & Ferland, 1999, Fig. 5)

Dependence of line ratios and cloud equilibrium temperature onto the slope of the irradiating power law.

Line Diagnostics, I

Before performing detailed spectral analysis of AGN spectra we need to understand how the physical properties of the emitting gas are determined.

- Density
- Temperature
- Mass

To get a fi rst estimate for these parameters, full blown photoionization computations are not necessary

$\Longrightarrow$ Line diagnostics.

Line Diagnostics, II

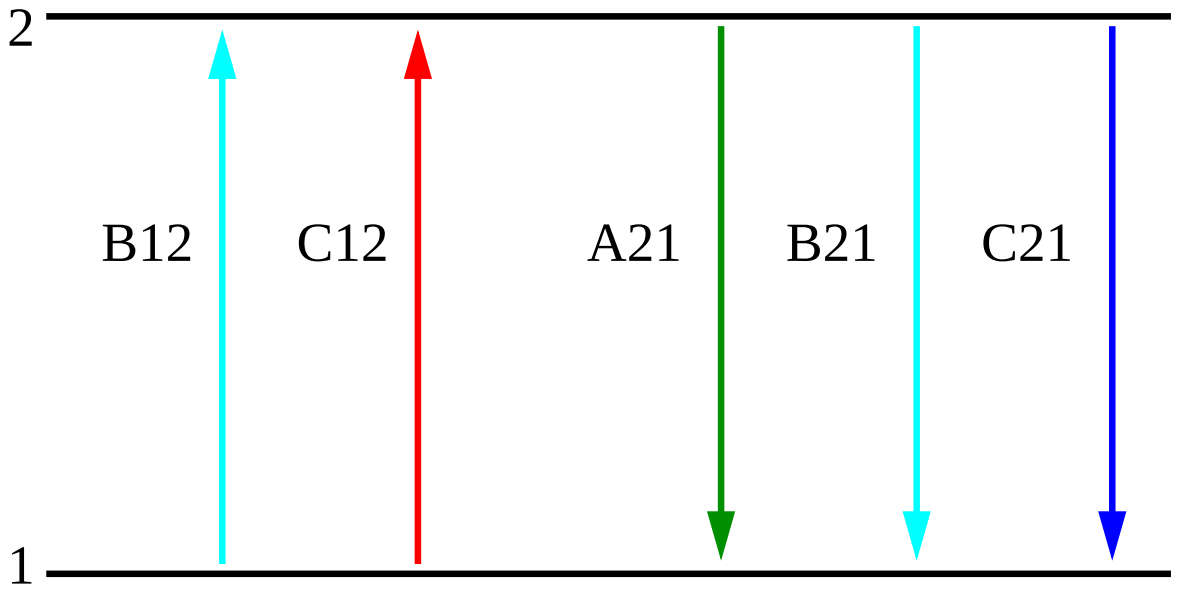

Line diagnostics makes use of (de)excitation mechanisms for line emission:

- Collisional Excitation, C_{12}
- Radiative Deexcitation, A_{21}
- Collisional Deexcitation, C_{21}

Coefficients for stimulated emission, B_{21}, and for radiative excitation (=absorption), B_{21}, can generally be ignored

Collisional (De)Excitation, I

Computation of C_{ij}:

For excitation, overall upwards rate is given by

$$R_{12} = n_e n_1 C_{12} = n_e n_1 \int_{E_{12}}^{\infty} \sigma_{12}(E) E f(E) \mathrm{d}E \tag{7.21}$$

where

- σ_{12}: collisional cross section
- $f(E)$: electron velocity distribution

σ_{12} varies roughly $\propto E^{-1}$. It can be parameterized as

$$\sigma_{12}(E) = \left(\frac{h^2}{8\pi m_e E}\right)\left(\frac{\Omega_{12}}{g_1}\right) \tag{7.22}$$

where Ω_{12} is called the collision strength and obtained from quantum mechanics (Seaton, 1958):

$$\Omega_{ij} = \left(\frac{8\pi}{\sqrt{3}}\right)\frac{g f_{ij}}{E_{ij}} \cdot G(T) \tag{7.23}$$

where $G(T)$ is a Gaunt factor.

Collisional (De)Excitation, II

Using the information from the previous slide and assuming a Maxwell-Boltzmann distribution for f, the upwards rate is

$$R_{12} = n_{\mathrm{e}} n_1 \left(\frac{2\pi\hbar^4}{k_{\mathrm{B}} m_{\mathrm{e}}^3}\right)^{1/2} T^{-1/2} \left(\frac{\Omega_{12}}{g_1}\right) \exp\left(-\frac{E_{12}}{kT}\right) \tag{7.24}$$

Analoguously, the rate for collisional de-excitation is

$$R_{21} = n_{\mathrm{e}} n_1 \int_0^\infty \sigma_{12}(E) E f(E) \mathrm{d}E \tag{7.25}$$

$$= n_{\mathrm{e}} n_2 \left(\frac{2\pi\hbar^4}{k_{\mathrm{B}} m_{\mathrm{e}}^3}\right)^{1/2} T^{-1/2} \left(\frac{\Omega_{21}}{g_2}\right) \tag{7.26}$$

as for de-excitation the energy threshold is zero.

Collisional (De)Excitation, III

To derive Ω_{21} in terms of Ω_{12}, make use of microreversibility:

In equilibrium, we know that the population densities are given by the Boltzmann distribution:

$$\frac{n_2}{n_1} = \frac{g_2}{g_1} \exp\left(-\frac{E_{12}}{kT}\right) \tag{7.27}$$

where g_1, g_2: statistical weights ($g = 2l + 1$).

But in equilibrium, by defi nition the upwards and downwards rate are the same:

$$R_{12} = R_{21} \tag{7.28}$$

such that

$$\frac{n_2}{n_1} = \left(\frac{\Omega_{12}}{g_1}\right)\left(\frac{g_2}{\Omega_{21}}\right) \exp\left(-\frac{E_{12}}{kT}\right) \tag{7.29}$$

and therefore

$$\Omega_{12} = \Omega_{21} \tag{7.30}$$

Line Diagnostics: Density, I

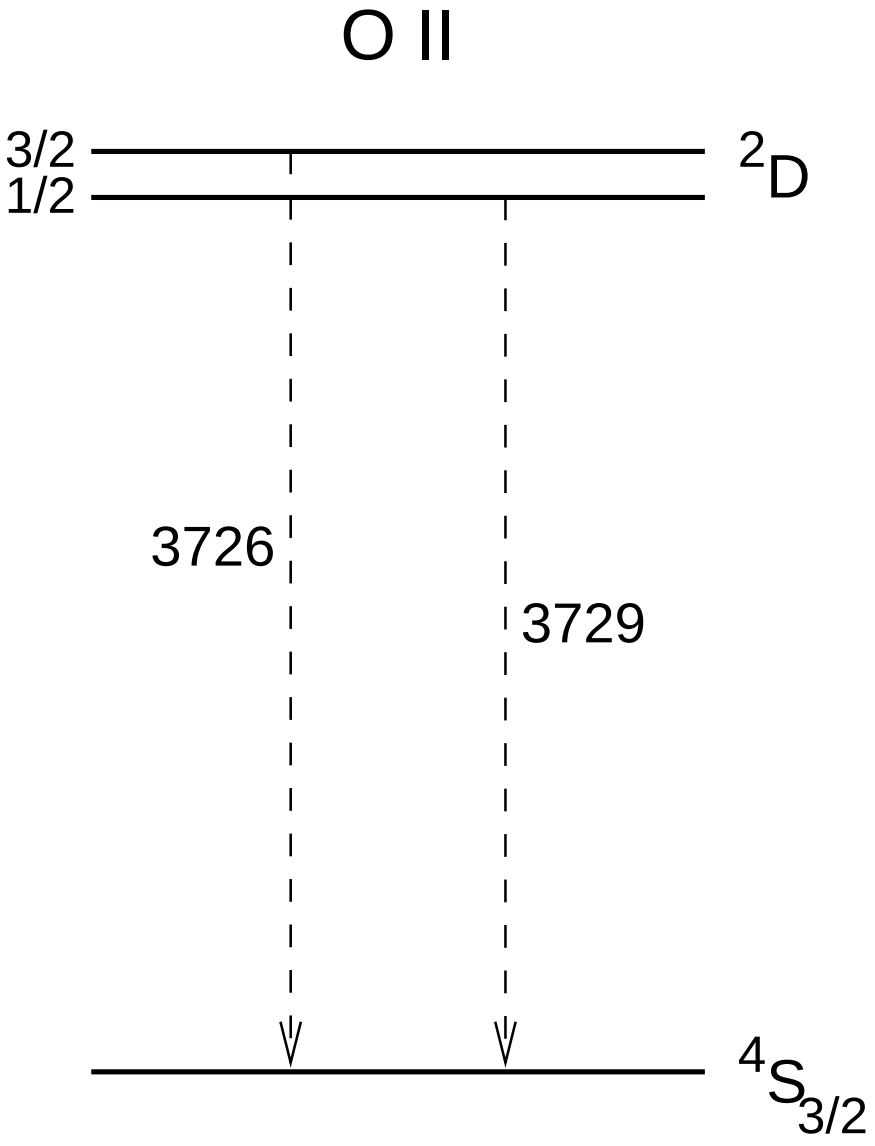

Density diagnostics: Choose atom with two levels with almost same excitation energy.

Excited ions then deexcite either radiatively or collisionally.

Line ratio between lines depends on rate of collisional deexcitations and thus is density dependent.

For $n_e \approx 1000\,\mathrm{cm}^{-3}$ use [OII] 3729/3726, for higher densities: CII

Line Diagnostics: Density, II

Rate equations in equilibrium:

$$n_1 n_e C_{12} = n_2 A_{21} + n_2 n_e C_{21} \tag{7.31}$$

$$n_1 n_e C_{13} = n_3 A_{31} + n_3 n_e C_{31} \tag{7.32}$$

such that

$$\frac{n_2}{n_1} = \frac{n_e C_{12}}{A_{21} + n_e C_{21}} = \frac{n_e}{A_{21} + n_e C_{21}} \frac{g_2}{g_1} C_{21} \exp(-E_{12}/kT) \tag{7.33}$$

$$\frac{n_3}{n_1} = \frac{n_e C_{13}}{A_{31} + n_e C_{31}} = \frac{n_e}{A_{31} + n_e C_{31}} \frac{g_3}{g_1} C_{31} \exp(-E_{13}/kT) \tag{7.34}$$

Assuming the cloud is optically thin (i.e., absorption is negligable), the intensity of an emitted line is

$$4\pi I_{21} = A_{21} n_2 h\nu_{21} \tag{7.35}$$

Line Diagnostics: Density, III

Using $4\pi I_{21} = A_{21} n_2 h\nu_{21}$, the line ratio is

$$\frac{I_{21}}{I_{31}} = \frac{A_{21} n_2 h\nu_{21}/4\pi}{A_{31} n_3 h\nu_{31}/4\pi} \tag{7.36}$$

since $\nu_{21} \sim \nu_{31}\ldots$

$$= \frac{A_{21} n_2}{A_{31} n_3} \tag{7.37}$$

insert n_2/n_3 from Eqs. (7.33) and (7.34)

$$= \frac{C_{21}}{C_{31}} \frac{g_2}{g_3} \frac{A_{21}}{A_{31}} \frac{A_{31} + n_e C_{31}}{A_{21} + n_e C_{21}} \exp(-E_{32}/kT) \tag{7.38}$$

$$= \frac{g_2 C_{21}}{g_3 C_{31}} \frac{1 + n_e/n_{Cr,3}}{1 + n_e/n_{Cr,2}} \exp(-E_{32}/kT) \tag{7.39}$$

where the critical densities are defi ned by

$$n_{Cr,i} = A_{i1}/C_{i1} \tag{7.40}$$

Line Diagnostics: Density, IV

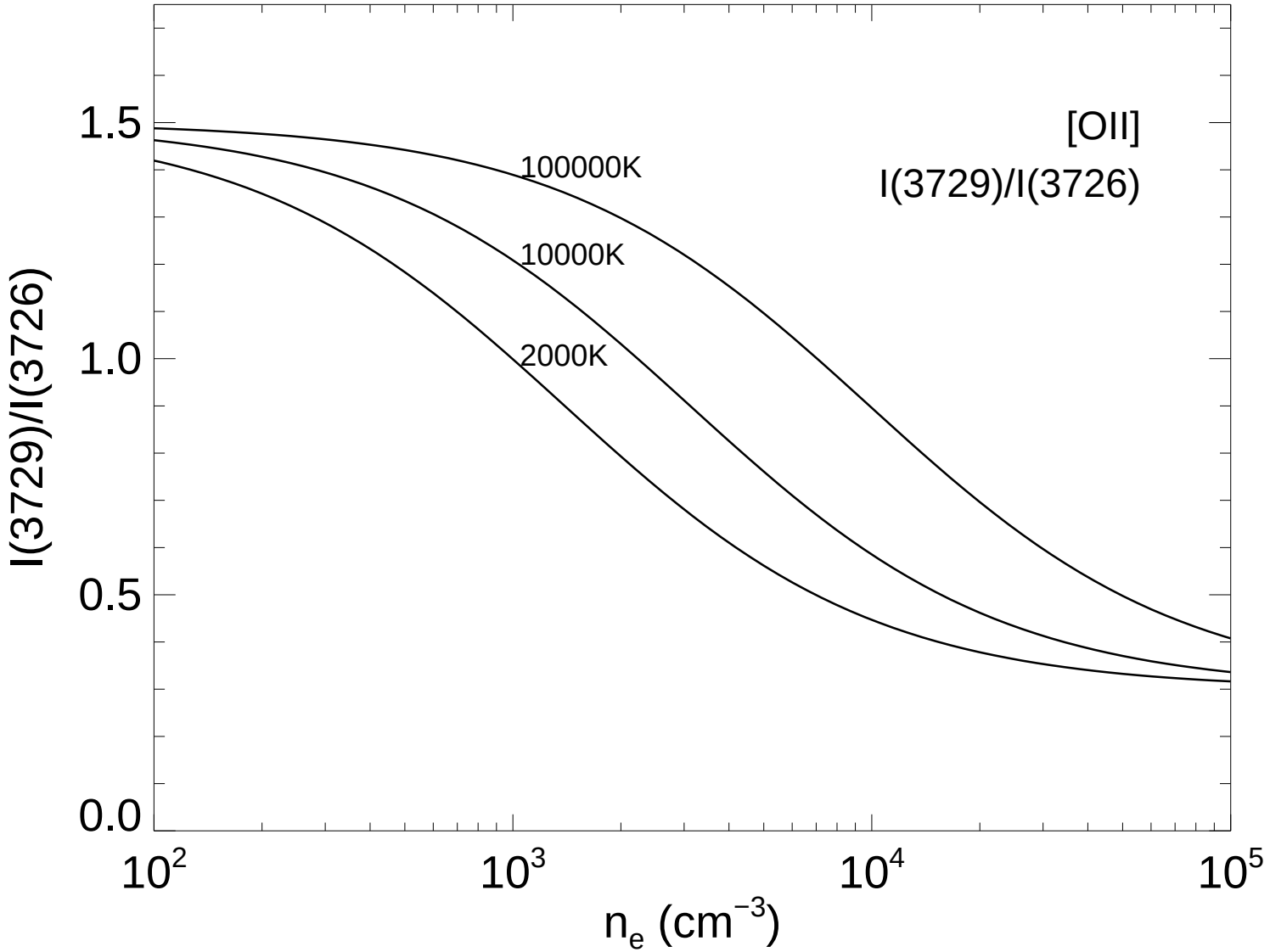

Note: Typical temperatures in AGN are $\sim 10^4$ K

Line Diagnostics: Density, V

Critical densities for $T = 10^4$ K used in AGN work (Hamann et al., 2002; Peterson, 1997).

Transition	$n_{\rm cr}\,({\rm cm}^{-3})$
[Ne III] λ3869	9.7×10^6
[Ne V] λ3426	1.60×10^7
C II] λ2326	3.16×10^9
C III λ977	1.59×10^{16}
C III] λ1909	1.03×10^{10}
C IV λ1549	2.06×10^{15}
[N I] λ5199	2×10^3
N II] λ2142	9.57×10^9
[N II] λ6548	8.7×10^4
[N II] λ6583	8.7×10^4
N III λ991	8.09×10^{15}
N III] λ1750	1.92×10^{10}
N IV] λ1486	5.07×10^{10}
N V λ1240	3.47×10^{15}

Transition	$n_{\rm cr}\,({\rm cm}^{-3})$
[O II] λ3727	4.5×10^3
O III λ834	2.14×10^{16}
[O III] λ4363	3.3×10^7
[O III] λ4959	7.0×10^5
[O III] λ5007	7.0×10^5
O III] λ1664	3.13×10^{10}
O IV λ789	1.17×10^{16}
O IV] λ1401	1.12×10^{11}
O VI λ1034	5.53×10^{15}
Si III] λ1892	3.12×10^{11}

Line Diagnostics: Temperature

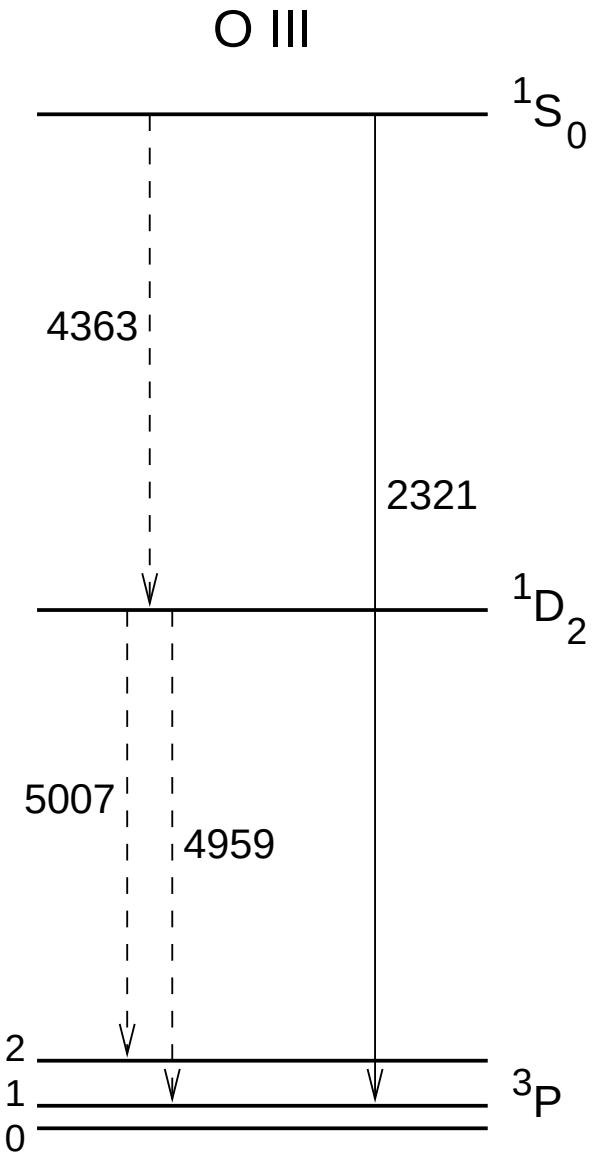

To obtain temperature use two levels with different excitation energy and make use of different collisional excitation probabilities for levels at different energies.

For $T \sim 10000\,\mathrm{K}$, mainly OIII and NII

Line Diagnostics: Temperature

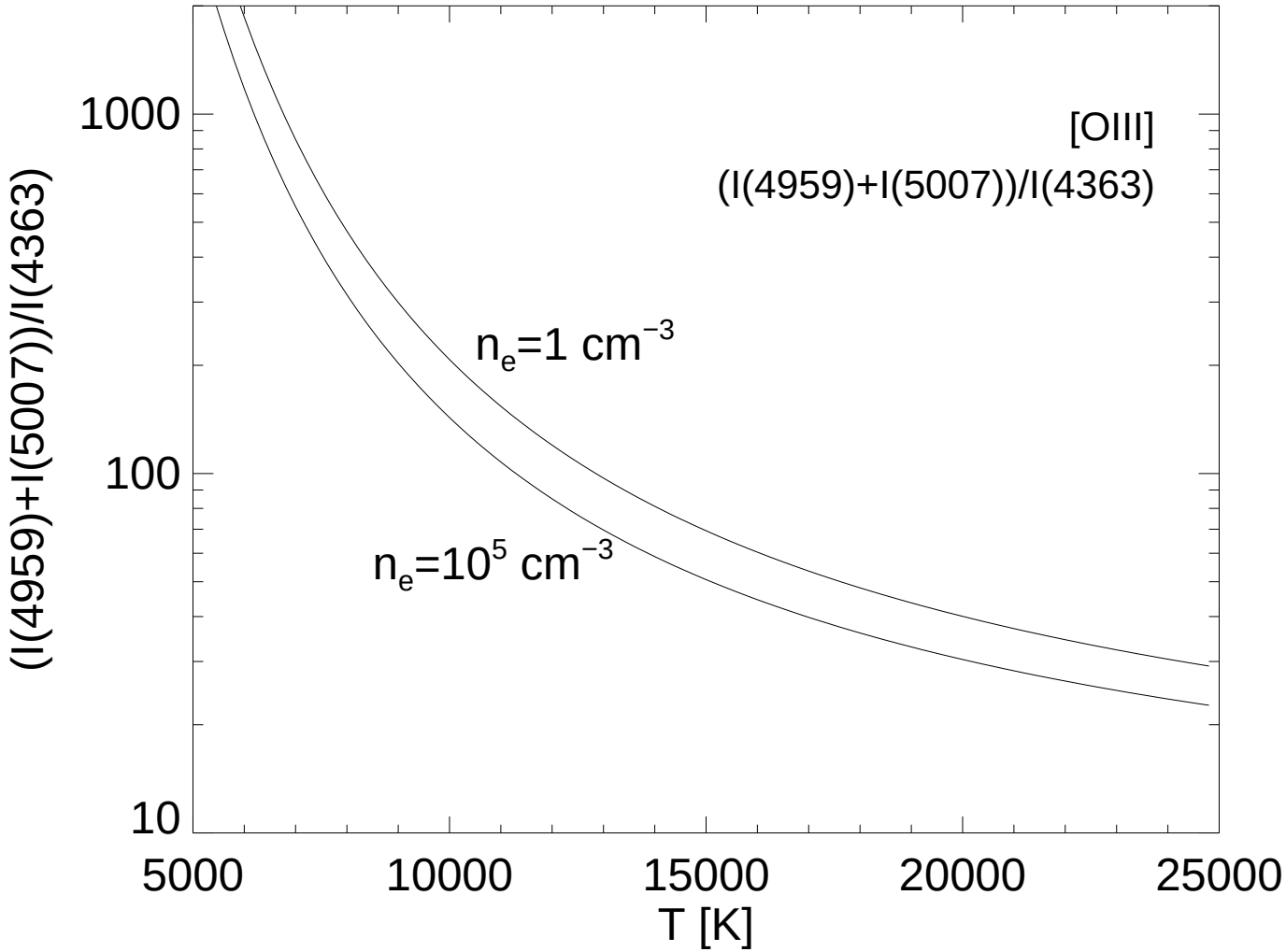

$$\frac{I(4959+5007)}{4363} = \frac{7.7\exp(3.29\times10^4/T)}{1+4.5\times10^{-4}n_{\rm e}T^{-1/2}}$$

Arnaud, M., & Rothenflug, R., 1985, A&AS, 60, 425

Ferland, G. J., & Mushotzky, R. F., 1982, ApJ, 262, 564

Francis, P. J., Hewett, P. C., Foltz, C. B., Chaffee, F. H., Weymann, R. J., & Morris, S. L., 1991, ApJ, 373, 465

Hamann, F., & Ferland, G., 1999, ARA&A, 37, 487

Hamann, F., Korista, K. T., Ferland, G. J., Warner, C., & Baldwin, J., 2002, ApJ, 564, 592

Karzas, W. J., & Latter, R., 1961, ApJS, 6, 167

Korista, K. T., & Ferland, G. J., 1989, ApJ, 343, 678

Mathews, W. G., & Ferland, G. J., 1987, ApJ, 323, 456

Menzel, D. H., & Pekeris, C. L., 1935, MNRAS, 96, 77

Nahar, S. N., Pradhan, A. K., & Zhang, H. L., 2001, ApJS, 133, 255

Osterbrock, D. E., 1989, Astrophysics of gaseous nebulae and active galactic nuclei, (Mill Valley, CA: University Science Books)

Peterson, B. M., 1997, An Introduction to Active Galactic Nuclei, (Cambridge: Cambridge Univ. Press)

Seaton, M. J., 1958, Rev. Mod. Phys., 30, 979

Shull, J. M., & Van Steenburg, M., 1982, ApJS, 48, 95

Verner, D. A., Ferland, G. J., Korista, K. T., & Yakovlev, D. G., 1996, ApJ, 465, 487

Verner, D. A., & Yakovlev, D. G., 1995, A&AS, 109, 125

Wilms, J., Allen, A., & McCray, R., 2000, ApJ, 542, 914